NUMERICAL INVESTIGATION OF COLLISION-INDUCED BREAKUP OF RAINDROPS. PART II: PARAMETERIZATIONS OF COALESCENCE EFFICIENCIES AND FRAGMENT SIZE DISTRIBUTIONS

Winfried Straub†, Jan Schlottke*, Klaus D. Beheng† and Bernhard Weigand*

† Institut für Meteorologie und Klimaforschung, Universität Karlsruhe / Forschungszentrum Karlsruhe
Hermann-von-Helmholtz-Platz 1, 76344 Eggenstein-Leopoldshafen, Germany

∗ Institut für Thermodynamik der Luft- und Raumfahrt, Universität Stuttgart
Pfaffenwaldring 31, 70569 Stuttgart, Germany

1 INTRODUCTION

Up to now, collision-induced breakup of raindrops has only been investigated in laboratory experiments with very limited sample of colliding drops of different sizes. McTaggart-Cowan and List (1975), Low and List (1982a) [abbreviated by LL82a] and Low and List (1982b) [abbreviated by LL82b], for example, derived coalescence efficiencies and numbers and size distributions of fragment drops resulting from collision-induced breakup from laboratory experiments with ten different pairs of large raindrops. Ochs et al. (1986) deduced coalescence efficiencies from experiments with ten different pairs of small precipitation drops and Ochs et al. (1995) and Beard and Ochs (1995) [abbreviated by BO95] investigated collision-induced breakup from experiments with four different pairs of drops. From their laboratory experiments, LL82a,b and BO95 developed parameterizations of coalescence efficiencies and size distributions of breakup fragments that are the one most frequently applied in meteorological cloud simulation models.

Recently, Beheng et al. (2006) [abbreviated by BE06] applied the VOF (Volume-of-Fluid) code FS3D (free surface 3D) model developed at the Institute of Aerospace Thermodynamics in Stuttgart, Germany to perform direct numerical simulations of collision-induced breakup of raindrops enlarging the database of LL82a,b to some 18 different pairs of colliding raindrops. The present study proceeds with the work of BE06 expanding the database to some 32 different pairs of drops. The model and setup as well as first results are explained in detail and compared with the findings of LL82a,b in Schlottke et al. (2008).

2 SIMULATION RESULTS

Overall, 32 drop pairs of sizes d_L (large drops) and d_S (small drops) are investigated. The drop pairs and sizes are listed in Tab. 1. The first ten drop pairs are identical to those investigated by LL82a,b and the first 18 drop pairs are identical to those of BE06. For each drop pair, six simulations are carried out. The simulations for each drop pair differ in the initial horizontal distance of the colliding drops, described by the excentricity ε that is the ratio of the horizontal distance δ of the droplet centers to the arithmetic mean of their diameters $\varepsilon = 2\delta/(d_L + d_S)$. Excentricities $\varepsilon = 0.05, 0.2, 0.4, 0.6, 0.8, 0.95$ have been chosen. Each simulation represents the collision results occuring in an individual segment of the cross section of size $\varepsilon\Delta\varepsilon$. The appropriate intervals $\Delta\varepsilon$ are $\Delta\varepsilon = 0.1, 0.2, 0.2, 0.2, 0.2, 0.1$. From this, the average number $\bar{f}$ of droplets is given as a weighted mean $\bar{f} = \sum n\varepsilon\Delta\varepsilon / \sum \varepsilon\Delta\varepsilon$ where n denotes the overall number of resulting drops per simulation. Similarly, coalescence efficiency E_c is given as fraction of the sum of cross section segments in which only coalescence occur to the sum of all cross section segments $E_c = \sum \delta_c \varepsilon\Delta\varepsilon / \sum \varepsilon\Delta\varepsilon$. In case of coalescence, that is, only one drop results from collision, $\delta_c = 1$, else $\delta_c = 0$. Now, the mean number $\bar{f}_b$ of breakup fragments is obtained from $\bar{f} = \bar{f}_b(1 - E_c) + E_c$. The results for E_c and $\bar{f}_b$ for all 32 drop pairs are also displayed in Tab. 1.

Besides this, the average number $\bar{p}_j(D_j)\Delta D_j$ of resulting droplets in the jth diameter intervall is needed. Here, $\bar{p}_j(D_j)$ denotes the average spectral number of drops in the jth diameter intervall with mean diameter D_j and ΔD_j denotes the width of the jth diameter intervall. As above, we

No.	d_L [cm]	d_S [cm]	Simulated E_c	Simulated $\bar{f}_b$	Calculated E_c	Calculated F_b
1	0.18	0.0395	0.49	2.00	0.60	2.00
2	0.40	0.0395	0.81	2.00	0.77	2.00
3	0.44	0.0395	0.81	2.00	0.80	2.00
4	0.18	0.0715	0.25	2.00	0.24	2.00
5	0.18	0.10	0.25	2.00	0.23	2.00
6	0.30	0.10	0.25	3.28	0.11	3.36
7	0.36	0.10	0.25	5.20	0.13	4.26
8	0.46	0.10	0.25	5.84	0.21	5.32
9	0.36	0.18	0.00	4.95	0.07	6.40
10	0.46	0.18	0.00	8.21	0.06	11.23
11	0.06	0.035	1.00	0.00	0.89	2.00
12	0.12	0.035	0.49	2.00	0.68	2.00
13	0.12	0.06	0.25	2.00	0.46	2.00
14	0.25	0.0395	0.49	2.00	0.65	2.00
15	0.24	0.09	0.25	2.00	0.14	2.07
16	0.27	0.15	0.09	2.79	0.11	3.12
17	0.32	0.0395	0.81	2.00	0.71	2.00
18	0.41	0.14	0.09	8.59	0.07	7.64
19	0.24	0.06	0.30	2.00	0.33	2.00
20	0.30	0.07	0.30	2.86	0.27	2.02
21	0.36	0.07	0.42	3.00	0.33	2.41
22	0.45	0.07	0.49	3.00	0.43	2.81
23	0.12	0.10	0.49	2.00	0.84	2.00
24	0.41	0.10	0.25	6.48	0.17	4.86
25	0.25	0.12	0.09	2.53	0.10	2.68
26	0.30	0.12	0.09	3.85	0.08	3.95
27	0.36	0.12	0.09	3.49	0.08	5.25
28	0.46	0.12	0.25	6.16	0.13	6.84
29	0.36	0.14	0.09	4.90	0.06	6.24
30	0.18	0.16	1.00	0.00	0.87	2.00
31	0.41	0.16	0.01	9.60	0.06	8.62
32	0.25	0.18	0.25	2.75	0.34	2.00

Table 1: *Coalescence efficiencies E_c and average numbers of breakup fragments $\bar{f}_b$, F_b as simulated with FS3D and calculated through the parameterization schemes developed in the following sections. Simulated and calculated coalescence efficiencies are correlated with correlation coefficient $r = 0.92$, simulated and calculated fragment numbers are correlated with $r = 0.93$.*

have $\bar{p}_j(D_j)\Delta D_j = \sum n_j \varepsilon\Delta\varepsilon / \sum \varepsilon\Delta\varepsilon$ with the overall number n_j of resulting drops per simulation within the jth diameter intervall. The average number $\bar{p}_{b,j}(D_j)\Delta D_j$ of breakup fragments is obtained from $\bar{p}_j(D_j)\Delta D_j = \bar{p}_{b,j}(D_j)\Delta D_j(1-E_c) + \delta(D_c)E_c$ with diameter of the coalesced drop $D_c = (d_L^3 + d_S^3)^{1/3}$. $\delta(D_c) = 1$ if D_c lies within the jth diameter intervall $|D_c - D_j| \leq \Delta D_j/2$, $\delta(D_c) = 0$ in all other cases.

3 COALESCENCE EFFICIENCIES

Coalescence efficiency is defined as the ratio of the number of collisions resulting in a permanent unification to the number of all collisions. In case of coalescence, the total energy E_T of coalescence must be dissipated by the coalesced drop, where E_T is the sum $E_T = CKE + \Delta S$ of the collision kinetic energy CKE and the energy ΔS resulting from net loss of surface area during unification with the incident drops. Collision kinetic energy CKE is given as

$$CKE = \frac{\pi}{12}\rho_l \frac{d_L^3 d_S^3}{d_L^3 + d_S^3}(v_L - v_S)^2 \qquad (1)$$

where ρ_l is the bulk density of water and v_L and v_S are the terminal fall velocities of the large and small drops. ΔS denotes the decrease of surface energy $\Delta S = S_T - S_C$. S_T denotes the total surface energy $S_T = \pi\sigma(d_L^2 + d_S^2)$ of the colliding drops and S_C is the surface energy $S_C = \pi\sigma(d_L^3 + d_S^3)^{2/3}$ of the coalesced system, σ is the surface tension of water.

For small d_S-values, the total energy E_T is small too, that is, in case of coalescence only a small amount of energy has to be dissipated. Thus, in this case we may assume that coalescence efficiency is large. Furthermore, numerical simulations with FS3D have shown that coalescence occurs much more often in case of small excentricities ε but only if the collision kinetic energy CKE is not too large. In case of large CKE almost all collisions result in breakup, i.e. coalescence efficiency tends to zero. The third case we have to pay attention for is the one occuring when the large and small incident drops are almost equal in size. In this case, CKE disappers but ΔS does not. We may assume that ΔS can be dissipated by the coalesced drop and we have coalescence. Simulations No. 11 and

30 support this argument. On the other hand, it is not clear if in this case we have to expect rebound that may not be simulated properly by the employed VOF method.

Taking the previous arguments into account, we approximate the simulated coalescence efficiencies by the exponential function $\exp(-We)$ where We denotes the Weber number

$$We = \frac{CKE}{S_C} \tag{2}$$

Now, the exponential function is equal to one for $CKE = 0$ and tends to zero for large Weber numbers. The best fitting expression is

$$E_c = \exp(-1.15We) \tag{3}$$

and is displayed in Fig. 1 and 2. In Fig. 1, the experimental results from LL82a are also included.

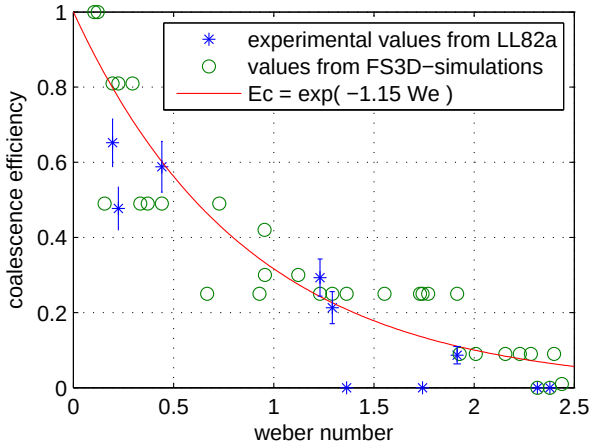

Fig. 1: *Coalescence efficiency E_c as function of the Weber number We. The correlation coefficient between the values from FS3D-simulations and the new parameterization is $r = 0.92$.*

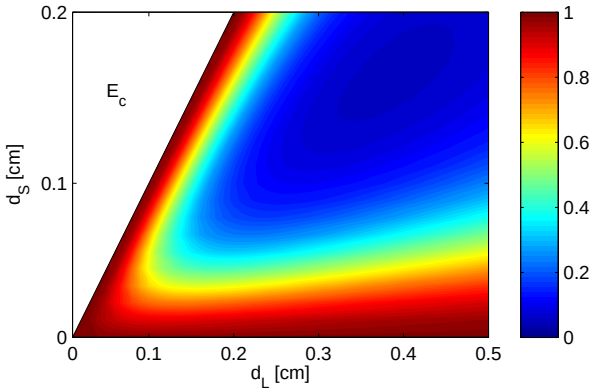

Fig. 2: *E_c-isolines (values see color bar) as function of colliding drop pairs with diameters d_L and d_S.*

4 SIZE DISTRIBUTIONS

In this chapter, a parameterization is developed to calculate the size distributions of breakup fragments as function of fragment diameters for several collisions of drops of sizes d_L and d_S. From the simulation results, four different modes of breakup fragments are identified.

- The first mode denoted by 'i' characterizes drops of sizes near d_L,
- the second mode 'ii' contains drops of sizes near d_S,
- the third mode 'iii' describes slightly smaller drops and
- the fourth mode 'iv' contains drops of smallest sizes.

The average number of drops found in each mode is given through $A_j = \bar{p}_{b,j}(D_j)\Delta D_j$ with the average spectral number $\bar{p}_{b,j}(D_j)$, the mean diameter D_j and the width ΔD_j of each mode as explained in chapter 2. Histograms for each collision of drops of sizes d_L and d_S are depicted in Fig. 6.

In our new parameterization, the fourth mode is characterized through a log-normal distribution reading

$$p_{\mathrm{iv}}(D) = \frac{1}{D\sigma_{\mathrm{iv}}\sqrt{2\pi}} \exp\left(-\frac{(\ln(D)-\mu_{\mathrm{iv}})^2}{2\sigma_{\mathrm{iv}}^2}\right) \tag{4}$$

where

$$\int_0^\infty p_{\mathrm{iv}}(D)\, dD = 1 \tag{5}$$

From this, the average spectral number $P_{\mathrm{iv}}(D)$ of fragments of the fourth mode is given as

$$P_{\mathrm{iv}}(D) = A_{\mathrm{iv}} p_{\mathrm{iv}}(D) \tag{6}$$

The parameters σ_{iv} and μ_{iv} can be expressed as

$$\sigma_{\mathrm{iv}}^2 = \ln\left(\frac{Var}{E^2}+1\right) \tag{7}$$

$$\mu_{\mathrm{iv}} = \ln(E) - \frac{\sigma_{\mathrm{iv}}^2}{2} \tag{8}$$

where E and Var denote the mean and variance of the log-normal distribution. On the other hand,

E and Var can be derived from the simulation results as $E = D_{iv}$ and $Var = \Delta D_{iv}^2/12$. From the simulations D_{iv} is approximated by a constant value = 0.04 cm and A_{iv} and ΔD_{iv} are approximated as

$$A_{iv} = \begin{cases} 0.75(E_T - 2.4) & \text{for} \quad E_T \geq 2.4\mu J \\ 0 & \text{for} \quad E_T < 2.4\mu J \end{cases} \tag{9}$$

$$\Delta D_{iv} = \begin{cases} k\left(\sqrt{E_T^2/S_C} - 1\right) & \text{for} \quad E_T^2/S_C \geq 1\mu J \\ 0 & \text{for} \quad E_T^2/S_C < 1\mu J \end{cases} \tag{10}$$

where $k = 1.7 \times 10^{-2}$ and E_T and S_C are given in μJ, ΔD_{iv} is given in cm. Simulated and calculated A_{iv} and ΔD_{iv} are correlated with correlation coefficients $r = 0.91$ and $r = 0.93$. The dependencies of simulated and calculated A_{iv} and ΔD_{iv} from E_T and E_T^2/S_C are shown in Fig. 3.

The third mode is characterized through a normal distribution

$$p_{iii}(D) = \frac{1}{\sigma_{iii}\sqrt{2\pi}}\left(-\frac{1}{2}\left(\frac{D - \mu_{iii}}{\sigma_{iii}}\right)^2\right) \tag{11}$$

where

$$\int_{-\infty}^{\infty} p_{iii}(D)\, dD = 1 \tag{12}$$

Now, the average spectral number $P_{iii}(D)$ of fragments of the third mode is given as

$$P_{iii}(D) = A_{iii}\, p_{iii}(D) \tag{13}$$

Here, $\mu_{iii} = D_{iii}$ and $\sigma_{iii}^2 = \Delta D_{iii}^2/12$. Again, from simulations D_{iii} is approximated as a constant with value $D_{iii} = 0.095$ cm and A_{iii} and ΔD_{iii} are approximated as

$$A_{iii} = 2.7 \times 10^{-6}\left(E_T^2/S_C\right)^4 \tag{14}$$

$$\Delta D_{iii} = 8.4 \times 10^{-8}\left(E_T^2/S_C\right)^4 \tag{15}$$

E_T and S_C are given in μJ, ΔD_{iii} is given in cm. In both cases, simulated and calculated A_{iii} and ΔD_{iii} are correlated with correlation coefficients $r = 0.96$. The dependencies of simulated and calculated A_{iii} and ΔD_{iii} from E_T^2/S_C are shown in Fig. 4.

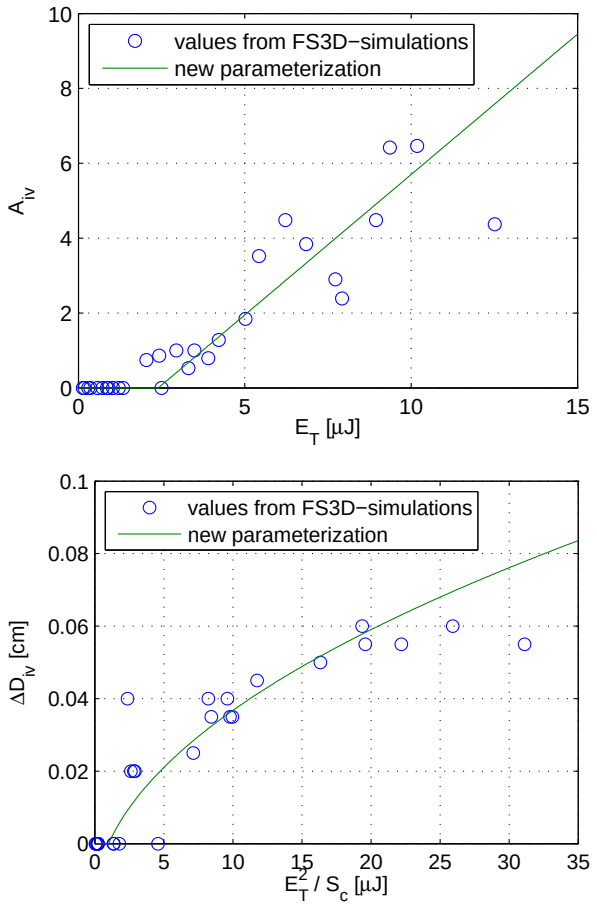

Fig. 3: *Parameters A_{iv} and ΔD_{iv} from simulations as well as from parameterization equations* (9) *and* (10) *as functions of E_T and E_T^2/S_C. The correlation coefficients between the values from FS3D-simulations and the new parameterization are $r = 0.91$ and $r = 0.93$.*

As for the third mode, the second mode is characterized through a normal distribution again

$$p_{ii}(D) = \frac{1}{\sigma_{ii}\sqrt{2\pi}}\left(-\frac{1}{2}\left(\frac{D - \mu_{ii}}{\sigma_{ii}}\right)^2\right) \tag{16}$$

In this case, the average spectral number $P_{ii}(D)$ of fragments of the second mode is

$$P_{ii}(D) = A_{ii}\, p_{ii}(D) \tag{17}$$

From simulations the mean diameter is approximately $D_{ii} = d_S - 0.01$ cm. A_{ii} and ΔD_{ii} are approximated as

$$A_{ii} = \begin{cases} 1 - h\left(E_T^2/S_C\right)^4 & \text{for} \quad E_T^2/S_C \leq 32,0\mu J \\ 0 & \text{for} \quad E_T^2/S_C > 32,0\mu J \end{cases} \tag{18}$$

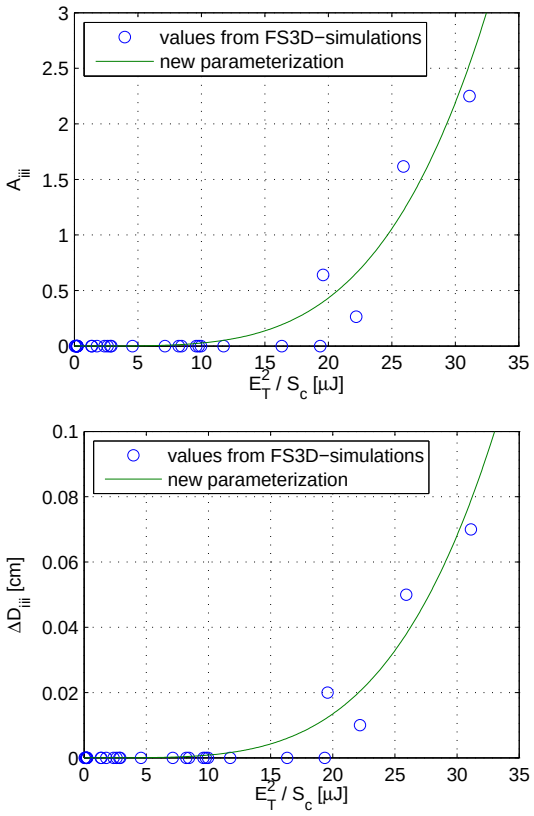

Fig. 4: *Parameters A_{iii} and ΔD_{iii} from simulations as well as from parameterization equations* (14) *and* (15) *as functions of E_T^2/S_C. The correlation coefficients between the values from FS3D-simulations and the new parameterization are $r = 0.96$ in both cases.*

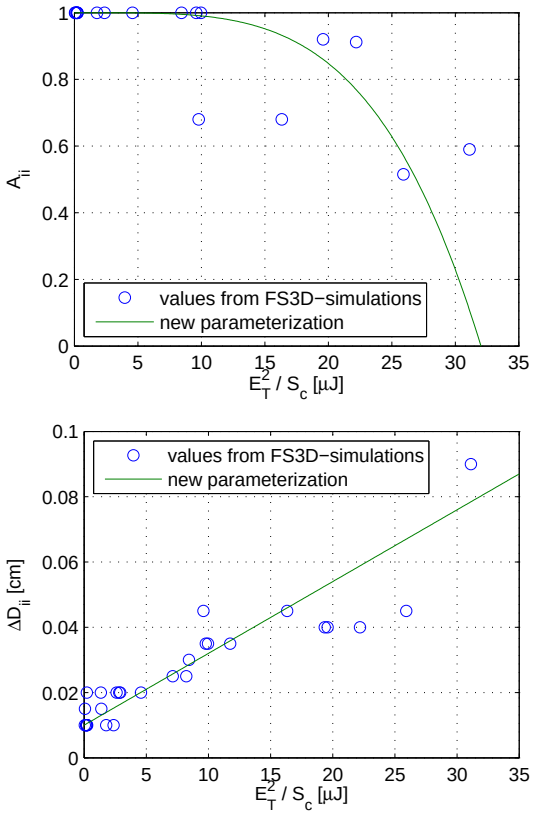

Fig. 5: *Parameters A_{ii} and ΔD_{ii} from simulations as well as from parameterization equations* (18) *and* (19) *as functions of E_T^2/S_C. The correlation coefficients between the values from FS3D-simulations and the new parameterization are $r = 0.73$ and $r = 0.91$.*

with $h = 9.5 \times 10^{-7}$ and

$$\Delta D_{\mathrm{ii}} = 1 \times 10^{-2} \left(0.22 E_T^2/S_C + 1\right) \qquad (19)$$

with E_T and S_C in μJ and ΔD_{ii} in cm. Simulated and calculated A_{ii} and ΔD_{ii} are correlated with correlation coefficients $r = 0.73$ and $r = 0.91$. The dependencies of simulated and calculated A_{ii} and ΔD_{ii} from E_T^2/S_C are shown in Fig. 5.

The first mode is characterized through a Dirac delta function $\delta(D - D_{\mathrm{i}})$ the integral of which is

$$\int_{-\infty}^{\infty} \delta(D - D_{\mathrm{i}})\, dD = 1 \qquad (20)$$

and the average spectral number $P_{\mathrm{i}}(D)$ of drops is $P_{\mathrm{i}}(D) = A_{\mathrm{i}}\delta(D - D_{\mathrm{i}})$. This results from the simulations showing that, in general, $A_{\mathrm{i}} = 1$. In order to ensure mass conservation D_{i} is derived from $D_{\mathrm{i}} = M_{3,\mathrm{i}}^{1/3}$ with $M_{3,\mathrm{i}}$ calculated as the residual of the masses of the two initial drops minus the masses of the drops from modes 'ii', 'iii' and 'iv':

$$M_{3,\mathrm{i}} = d_L^3 + d_S^3 - M_{3,\mathrm{iv}} - M_{3,\mathrm{iii}} - M_{3,\mathrm{ii}} \qquad (21)$$

where the moments M_3 on the r.h.s. are given according to their distribution functions assumed by

$$M_{3,\mathrm{iv}} = A_{\mathrm{iv}} \exp\left(3\mu_{\mathrm{iv}} + \frac{9\sigma_{\mathrm{iv}}^2}{2}\right) \qquad (22)$$

$$M_{3,\mathrm{iii}} = A_{\mathrm{iii}} \left(\mu_{\mathrm{iii}}^3 + 3\mu_{\mathrm{iii}}\sigma_{\mathrm{iii}}^2\right) \qquad (23)$$

$$M_{3,\mathrm{ii}} = A_{\mathrm{ii}} \left(\mu_{\mathrm{ii}}^2 + 3\mu_{\mathrm{ii}}\sigma_{\mathrm{ii}}^2\right) \qquad (24)$$

Note that in this way a single drop remains with a diameter only slightly smaller than d_L.

Now, the overall spectral number of breakup fragments is given as

$$P_b(D) = P_{\mathrm{iv}}(D) + P_{\mathrm{iii}}(D) + P_{\mathrm{ii}}(D) + P_{\mathrm{i}}(D) \qquad (25)$$

and is displayed in Fig. 6 at the end of the paper for all 30 cases of different drop pairs of sizes d_L

and d_S (in two cases coalescense efficiency is one, that is, no breakup fragments has been simulated). According to chapter 2, the average number of resulting drops is given by

$$P(D) = P_b(D)(1 - E_c) + \delta(D_c)E_c \qquad (26)$$

where $\delta(D_c) = 1$ if $D = D_c$ and $\delta(D_c) = 0$ in all other cases.

The average number F_b of all breakup fragments for each initial drop pair of size d_L and d_S is now obtained from

$$F_b = \int_0^\infty P_b(D)\, dD \qquad (27)$$

and is given in Tab. 1. The overall number F of all resulting drops is then $F = F_b(1 - E_c) + E_c$.

5 SUMMARY AND CONCLUSIONS

In the present study, collision-induced breakup is investigated by application of the numerical simulation code FS3D. New parameterizations of coalescence efficiency as well as size distributions of fragment drops are developed on an extended basis of 32 different pairs of colliding drops of sizes $0 < d_L < 0.5\,\text{cm}$ and $0 < d_S < 0.2\,\text{cm}$. Additionally, the new parameterization of coalescence efficiency fits quite well to the data of LL82a.

To increace accuracy of the parameterizations, further investigation should focus on increasing the number of simulations for each drop pair. Furthermore, it is needed to clarify the collision process for initial drop pairs of nearly the same size and to adjust the parameterization of coalescence efficiency to the new findings.

Acknowledgement

The authors gratefully acknowledge support by the German Science Foundation (DFG) under grants BE 2081/7-1 and WE 2549/17-1 in the framework of the priority program Quantitative Precipitation Forecast.

References

Beard, K. V. and H. T. Ochs (1995): Collisions between Small Precipitation Drops. Part II: Formulas for Coalescence, Temporary Coalescence, and Satellites. *J. Atmos. Sci.*, **52**, 3977–3996.

Beheng, K. D., K. Jellinghaus, W. Sander, N. Roth and B. Weigand (2006): Investigation of Collision-induced Breakup of Raindrops by Numerical Simulations: First Results. *Geophys. Res. Lett.*, **33**, L10811, doi:10.1029/2005GL025519.

Low, T. B. and R. List (1982a): Collision, Coalescence and Breakup of Raindrops. Part I: Experimentally Established Coalescence Efficiencies and Fragment Size Distributions in Breakup. *J. Atmos. Sci.*, **39**, 1591–1606.

Low, T. B. and R. List (1982b): Collision, Coalescence and Breakup of Raindrops. Part II: Parameterization of Fragment Size Distributions. *J. Atmos. Sci.*, **39**, 1607–1618.

McTaggart-Cowan, J. D. and R. List (1975): Collision and Breakup of Water Drops at Terminal Velocity. *J. Atmos. Sci.*, **32**, 1401–1411.

Ochs, H. T., K. V. Beard, R. R. Czys, N. F. Laird, D. E. Schaufelberger and D. J. Holdridge (1995): Collisions between Small Precipitation Drops. Part I: Laboratory Measurements of Bounce, Coalescence, and Temporary Coalescence. *J. Atmos. Sci.*, **52**, 2258–2275.

Ochs, H. T., R. R. Czys and K. V. Beard (1986): Laboratory Measurements of Coalescence Efficiencies for Small Precipitation Drops. *J. Atmos. Sci.*, **43**, 225–232.

Schlottke, J., W. Straub, K. D. Beheng and B. Weigand (2008): Numerical Investigation of Collision-induced Breakup of Raindrops. Part I: Methodology as well as Dependencies on Collision Energy and Excentricity. *15th International Conference on Clouds and Precipitation, July 7-11, 2008, Cacun, Mexico*.

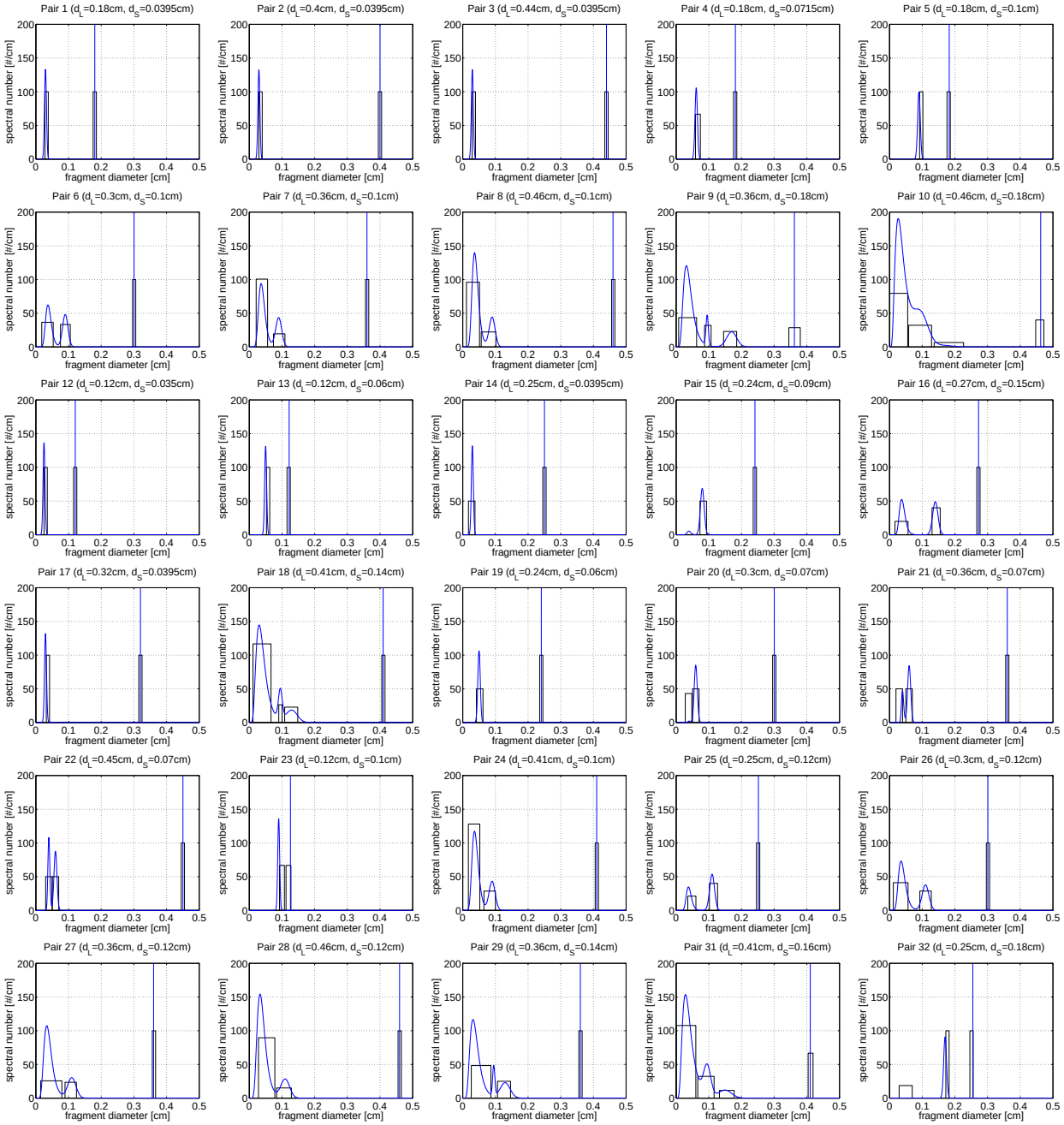

Fig. 6: *Spectral number of fragments as function of fragment diameter for d_S and d_L as indicated. Black boxes refer to the simulation results (cf. fig. 11 of the companion paper of Schlottke et al. (2008), this volume) and blue lines to the parameterizations for 30 different drop pairs. The first 10 pairs are the same as in LL82b. In case of pair 11 and pair 30 coalescence efficiency is one, that is, in these cases no breakup occurs.*